PHYSICAL REVIEW C **83**, 061305(R) (2011)

Triple configuration coexistence in ^{44}S

D. Santiago-Gonzalez,[1] I. Wiedenhöver,[1] V. Abramkina,[1] M. L. Avila,[1] T. Baugher,[2,3] D. Bazin,[2] B. A. Brown,[2,3] P. D. Cottle,[1] A. Gade,[2,3] T. Glasmacher,[2,3] K. W. Kemper,[1] S. McDaniel,[2,3] A. Rojas,[1] A. Ratkiewicz,[2,3] R. Meharchand,[2,3] E. C. Simpson,[4] J. A. Tostevin,[4] A. Volya,[1] and D. Weisshaar[2]

[1]*Department of Physics, Florida State University, Tallahassee, Florida 32306-4350, USA*

[2]*National Superconducting Cyclotron Laboratory, Michigan State University, East Lansing, Michigan 48824, USA*

[3]*Department of Physics and Astronomy, Michigan State University, East Lansing, Michigan 48824, USA*

[4]*Department of Physics, Faculty of Engineering and Physical Sciences, University of Surrey, Guildford, Surrey GU2 7XH, United Kingdom*

(Received 22 December 2010; revised manuscript received 24 March 2011; published 30 June 2011)

The neutron-rich $N = 28$ nucleus ^{44}S was studied using the two-proton knockout reaction from ^{46}Ar at intermediate beam energy. We report the observation of four new excited states, one of which is a strongly prolate deformed 4^+ state, as indicated by a shell-model calculation. Its deformation originates in a neutron configuration which is fundamentally different from the "intruder" configuration responsible for the ground-state deformation. Consequently, we do not have three coexisting shapes in ^{44}S, but three coexisting configurations, corresponding to zero-, one-, and two-neutron particle-hole excitations.

DOI: 10.1103/PhysRevC.83.061305 PACS number(s): 21.10.Pc, 21.60.Cs, 25.70.Hi, 27.40.+z

For 20 years, a primary focus of nuclear structure physics has been the search for the proposed modification of shell structure in nuclides near the neutron dripline [1–8]. The neutron shell closures at $N = 28$, 50, 82, and 126 are set by the spin-orbit splitting of high angular momentum orbits, so that a reduction in the splitting would result in the narrowing or collapse of one or more of these shell gaps. The modification of shell gaps has recently been discussed as due to two-body effective interactions of central and tensor type [9] and a decomposition into central, vector, and tensor forces [10]. At present, the only one of these spin-orbit-based neutron shell closures that is accessible to experiments close to the neutron dripline is $N = 28$. Admixtures of cross-shell configurations to the wave functions of neutron-rich $N = 28$ nuclei and the narrowing of the $N = 28$ gap were recently established experimentally [11–15].

Experimental investigations of how the narrowing of the $N = 28$ gap affects nuclear structure have focused on how two particle–two hole "intruder" configurations resulting from the promotion of a pair of neutrons across the $N = 28$ gap cause deformation in these nuclei. The recent study of the ground state and excited 0^+ state in ^{44}S [16] highlights the interaction between the "normal" configuration–in which the neutrons are confined to the orbits below the $N = 28$ gap—and the intruder configuration.

In this Rapid Communication we report on the observation of a 4^+ state at 2447 keV, populated via the two-proton knockout reaction from ^{46}Ar performed at intermediate energies, as well as three other states and five γ transitions that were previously unobserved. The spin and parity assignment for the 2447-keV state is made using the longitudinal momentum distribution of the projectile residues. A shell-model calculation performed using the new SDPF-U effective interaction [17] suggests that this state is strongly deformed and that the neutron configuration responsible for this deformation results from promotion of a single neutron across the $N = 28$ gap—a fundamentally different microscopic mechanism than that which causes deformation in the "intruder" 0^+ ground state. The shell-model calculation also provides a prediction that this deformed 4^+ state has a half-life of approximately 60 ps, giving it a character that is generally associated with the term "high-K isomer" in heavier nuclei. Thus, ^{44}S does not have three coexisting shapes, but three coexisting configurations, corresponding to zero-, one-, and two-neutron particle-hole excitations.

The present experiment was performed at the National Superconducting Cyclotron Laboratory at Michigan State University using the Coupled Cyclotron Facility (CCF). A beam of the radioactive isotope ^{46}Ar was produced via fragmentation of a primary beam of 140 MeV/nucleon ^{48}Ca provided by the CCF. The primary beam was fragmented on a 705 mg/cm^2 thick beryllium target, and the fragmentation products were separated in the A1900 fragment separator [18]. The separator selected a secondary beam of 99.9 MeV/nucleon ^{46}Ar which had a momentum spread of $\pm 1.3\%$ and a purity exceeding 90%. The rate of ^{46}Ar particles impinging on the secondary target averaged 7×10^5 particles/s.

The knockout reactions were induced on a secondary beryllium target of thickness 188 mg/cm^2. The residual projectile-like nuclei were detected in the S800 spectrograph [19]. Figure 1 shows the histogram of signals used to identify the reaction residues. Gamma rays emitted at the secondary target location were detected using the SeGA array of 17 segmented germanium detectors [20] in coincidence with the residues in the S800 spectrograph. The total photopeak efficiency of the SeGA array for γ rays emitted in-flight ($v/c = 0.4211$) was 2.5% at 1 MeV and 1.4% at 2 MeV.

The γ-ray spectrum in coincidence with the ^{44}S residual nuclei is shown in Fig. 2. These spectra are Doppler-reconstructed to the rest frames of the residual nuclei. The strongest γ ray in the spectrum is the 1319-keV line, which was first observed in 1997 by Glasmacher *et al.* in a measurement of the intermediate energy Coulomb excitation reaction [21] and assigned to be the $2^+_1 \rightarrow 0^+_{\text{g.s.}}$ transition. In addition, we observe γ rays at 949, 1128, 1891, 1929, and 2150 keV. The experimental uncertainties on the γ-ray energies are 0.5%.

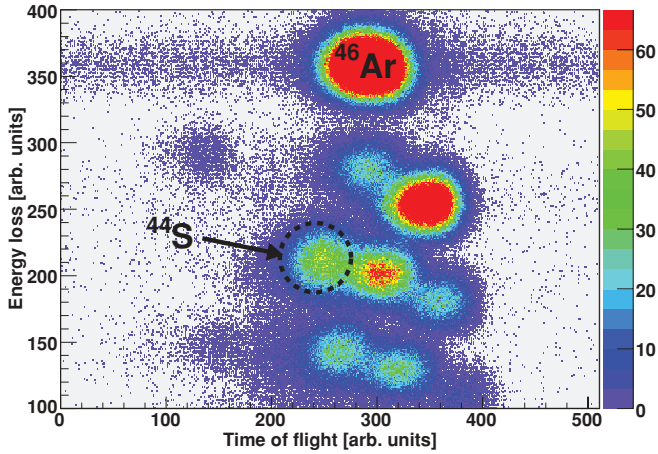

FIG. 1. (Color online) Spectrum of residual nuclei identified in the S800 spectrograph. The particles labeled ^{46}Ar correspond to scattered beam particles in the hydrogen-like charge state. The vertical axis displays the energy loss of nuclides measured in the focal plane, and the horizontal axis represents a path-corrected time-of-flight signal measured between a focal plane detector and the accelerator RF reference.

Figure 3 shows the spectrum of γ rays in coincidence with both the 1319-keV γ ray and the ^{44}S residues. This coincidence spectrum shows three of the peaks from Fig. 2, at 949, 1128, and 1929 keV. On this basis, we establish the existence of states at 2268, 2447, and 3248 keV. The coincidence spectra gated on the 949-, 1128-, and 1929-keV γ rays show no mutual coincidences. The level scheme we deduce is shown in Fig. 4.

Figure 2 also shows two γ rays at 1891 and 2150 keV that are not seen in the 1319-keV coincidence spectrum. With respect to the 1891-keV γ ray, we note that Force *et al.* [16] previously reported the observation of an isomeric 0^+ state at 1365(1) keV, which is 36 keV above the energy they assigned for the 2_1^+ state, 1329(1) keV. The only decay of this state would be to the ground state via the emission of conversion electrons, so this decay could not be observed in the present experiment. However, the 1891-keV γ ray is 38 keV lower in energy than the 1929-keV γ ray that deexcites the 3248-keV state. Hence, we tentatively assign the 1891-keV γ ray as a transition from the 3248-keV state to the 0_2^+ state proposed by

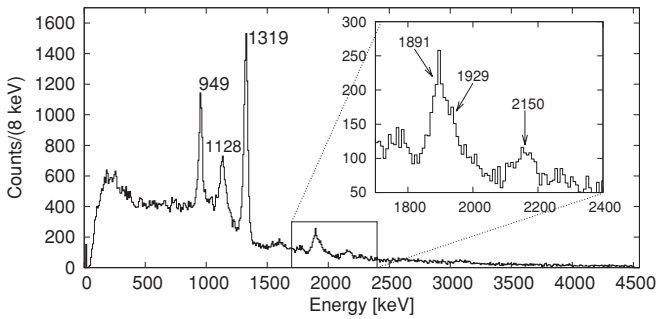

FIG. 2. Doppler-corrected ($v/c = 0.4211$) energy of γ rays detected in coincidence with the ^{44}S residues. Inset shows a closeup of the 1700–2400 keV region where three less intense photopeaks are identified.

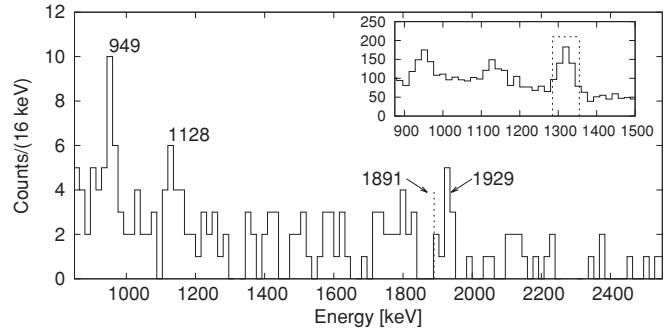

FIG. 3. Doppler-corrected energy of γ rays detected in coincidence with the 1319-keV γ rays emitted from a ^{44}S nucleus. Inset: Projected spectrum of $\gamma\gamma$ events showing energy coincidence window in dotted lines.

Force *et al.*. Within the statistical limits of our experiment, the 2150-keV γ ray is not coincident with other γ rays and is, thus, tentatively placed as populating the ground state. Table I lists the levels, γ rays deexciting the levels and the cross sections for populating these levels.

Sohler *et al.* published a level scheme for ^{44}S deduced from γ rays observed during the fragmentation of an intermediate energy beam of ^{48}Ca [22]. The only γ transition that is unambiguously common to the spectra of Sohler *et al.* and the present work is the $2_1^+ \rightarrow 0_{\text{g.s.}}^+$ transition, which Sohler quotes as 1350(10) keV and which is quoted as 1319(7) keV here. Sohler *et al.* also assign a 988(15)-keV transition to ^{44}S and say that it deexcites a state at 2632 keV. There is a 31-keV difference between the 2_1^+ state energies quoted here and by Sohler *et al.*, so it is possible that the 949(5)-keV γ ray observed here is identical to the 988(15)-keV γ ray reported by Sohler *et al.* However, if the two γ rays are identical, it is clear that the γ ray was misplaced in the level scheme in the previous study.

Longitudinal momentum distributions were extracted for residues in coincidence with the 949- and 1128-keV γ transitions, corresponding to the direct population of the 2268- and 2447-keV levels. In addition, a distribution was extracted for residues from direct population of the 1319-keV state by proportionally subtracting the distributions in coincidence with the 949- and 1128-keV γ transitions from the one in

TABLE I. Deduced energy levels of ^{44}S, E_{level}, with their spin and parity, J^π, measured deexcitation energy, E_γ, placed toward the final level. Experimental and theoretical cross sections for populating the levels are also listed (see text).

E_{level} (keV)	J^π	E_γ (keV)	J^π_{final}	σ (mb)	σ_{theory} (mb)
0	0^+				0.334
1319(7)	2_1^+	1319(7)	0_1^+	0.014(3)	0.028
1357(15)	0_2^+				0.163
2150(11)*	(2_2^+)	2150(11)	0_1^+*	0.004(1)	0.076
2268(8)	2_3^+	949(5)	2_1^+	0.022(4)	0.082
2447(9)	4_1^+	1128(6)	2_1^+	0.019(4)	0.032
3248(12)	(2_4^+)	1891(10)	0_2^+*	0.011(3)	0.033
		1929(7)	2_1^+		

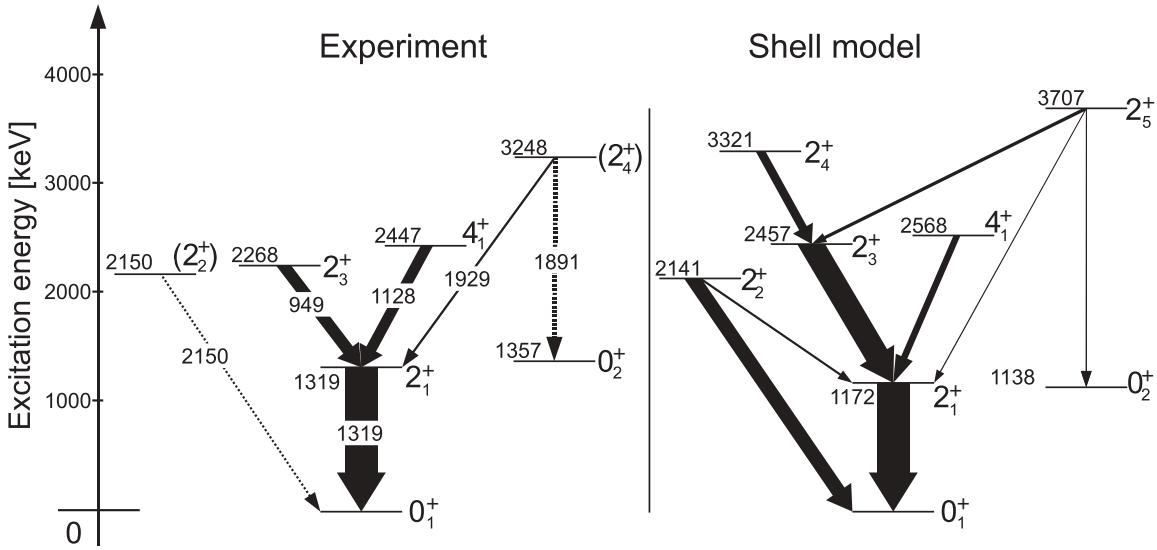

FIG. 4. (Left) Experimental ^{44}S level scheme. The arrow widths are proportional to the observed intensity of the transitions. (Right) Level and transition scheme predicted by the shell model (see text). The arrow widths represent the calculated γ intensities based on population cross sections and subsequent γ-decay branching ratios, normalized to the strength of the $2_1^+ \rightarrow 0_1^+$ transition. We show all predicted transitions calculated larger than 3% of the $2_1^+ \rightarrow 0_1^+$ transition intensity.

coincidence with the 1319-keV γ rays. In Fig. 5, the observed distributions are compared with those calculated for states of different J^π values, which were corrected for the broadening induced by beam particle and reaction residue energy losses in the target. The model used for calculating these distributions assumes sudden, direct two-proton removal reactions and combines eikonal dynamics and shell-model wave functions. These shell-model calculations were performed using the SDPF-U interaction [17], which was recently deduced from a fit to data on $Z = 8$–20 nuclei ranging from near-proton dripline to near-neutron dripline systems.

The reaction theory, first presented in Refs. [24,25] and extended in [26,27], demonstrates that the reaction dynamics restrict direct two-nucleon removal events to grazing collisions. In this way the collision samples the joint position and momentum configurations of the two removed nucleons [28]. Here, the shell-model calculations provide the two-proton amplitudes connecting the ground state of the parent nucleus (^{46}Ar) with the final states of the daughter nucleus (^{44}S). Both states are represented by their full shell-model wave functions, including cross-shell configurations. In general, a wider longitudinal momentum distribution indicates a higher total and orbital angular momentum transfer to the residual nucleus. The momentum distribution for the 1319-keV state is consistent with an assignment of 2^+ that was set in Ref. [21]. The observed distribution in coincidence with the 949-keV γ ray is also best reproduced by a 2^+ assignment for the 2268-keV state. However, the experimental distribution in coincidence with the 1128-keV γ ray indicates a 4^+ assignment for the 2447-keV state.

Figure 4 compares the states observed in the present experiment with predictions of the shell-model calculation. The experimental results are also listed in Table I. The calculation predicts five excited states below 2.7 MeV, in agreement with our observations. The predictions of γ-ray intensities, represented by arrow widths in Fig. 4 (right), are derived from the calculated cross sections for the direct population of the excited states and their corresponding γ-decay branches, where we used the effective charges $e_p = 1.5$ and $e_n = 0.5$ and the free-nucleon $M1$ operator.

The inclusive cross section of the two-proton knockout reaction is 0.23(2) mb, while the reaction model calculates 0.87 mb. These observed cross sections are smaller than those calculated with the shell model and reaction model. However, theoretical cross sections systematically overestimate experimental cross sections by a factor of 2 [25] and the present results do not deviate significantly from this reduction.

Table I also lists the individual experimental and calculated cross sections for the observed states. The ground state and the excited 0^+ states are calculated to carry more than 50% of the total cross section. Among the excited states populated in our experiment, the 2_3^+ and 4_1^+ carry the largest individual cross sections, larger than the 2_1^+, which, in agreement with the calculation, is populated mostly indirectly. The tentatively identified 2150-keV (2_2^+) state is only weakly populated, while the reaction model predicts a strong population.

The role of the two particle–two hole (2p-2h) neutron intruder configurations in inducing deformation in ^{44}S was first illustrated by Glasmacher *et al.* [21] who observed a large $B(E2\uparrow)$ value of 314(88) e^2 fm^4 [6.8(20) Weisskopf units], implying significant collectivity or permanent quadrupole deformation. The recent electron spectroscopy studies of Grevy *et al.* [23] and Force *et al.* [16] demonstrated that the 0_1^+ ground state and the excited 0_2^+ state represent a strongly mixed two-state system based on the prolate deformed intruder 2p-2h neutron configuration and spherical state originating in the normal neutron configuration.

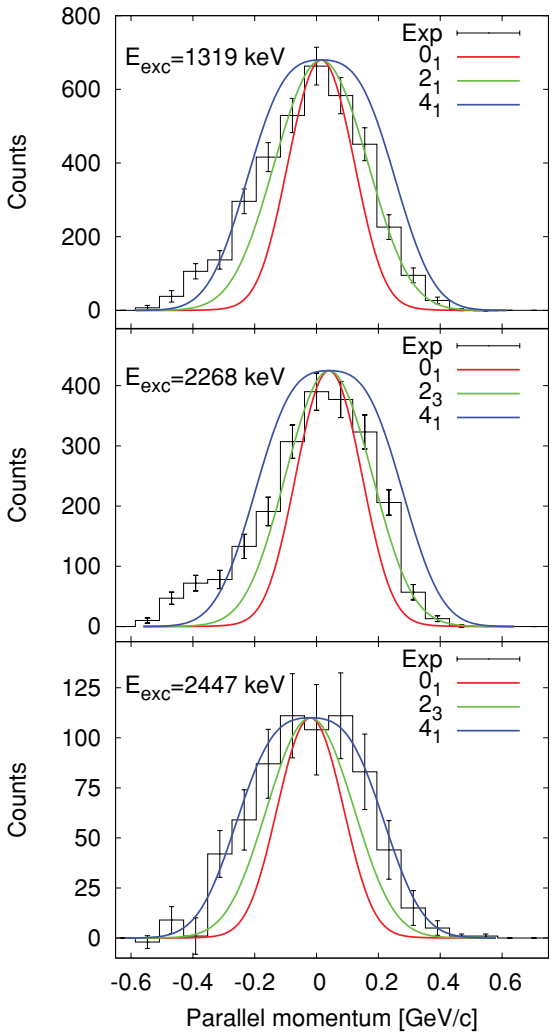

FIG. 5. (Color online) Calculated and observed longitudinal momentum distributions for the direct population of the 1319-keV state (2_1^+) (top), the 2268-keV state (2_3^+) (middle), and the 2447-keV state (4_1^+) (bottom). The experimental histogram is compared to the distributions calculated from the two-proton knockout mechanism for different final state spin hypotheses (see text), which were corrected for the broadening induced by beam particle and reaction residue energy losses in the target.

The shell-model calculation of this work gives a large laboratory frame electric quadrupole moment, 26 e fm^2, for the lowest 4^+ state observed in the present experiment. However, this 4^+ state is not connected to the deformed ground-state band by the strong $E2$ transitions that would be characteristic of in-band transitions. Instead, the calculation predicts that the 4^+ state is deexcited by a hindered $E2$ transition to the 2_1^+ so that it has a long lifetime—about 60 ps. In fact, in a heavier rotational nucleus this 4^+ state would be called a "high-K" isomer because it appears to be the bandhead of a $K = 4$ band. If we transform the shell-model result for the quadrupole moment of this state to an intrinsic frame (using a rotational model and the $K = 4$ hypothesis), we find that the intrinsic deformation is prolate with a magnitude of 51 e fm^2.

While the ground-state band is calculated with a prolate deformation as well, the microscopic origins of these prolate deformations are quite different. An examination of the lowest 4^+ state reveals that it is mainly based on 1p-1h neutron excitations, accounting for 59% of its wave-function, of which $(f_{7/2})^{-1} p_{3/2}$ is the leading configuration. By comparison, the rotational 2_1^+ and 4_2^+ shell-model states are dominated by 2p-2h excitations being 63% and 65% of their respective wave functions. It is interesting to note that the unobserved rotational 4_2^+ state is calculated to be populated with less than 1 μb of cross section. In the calculation, the 4_1^+ and the unobserved rotational 4_2^+ state are separated by only 164 keV, yet exhibit virtually no mixing, as demonstrated by the calculated long lifetime of the 4_1^+ state. Thus, we do not have three coexisting shapes in ^{44}S, but three coexisting configurations, corresponding to zero-, one-, and two-neutron particle-hole excitations.

The line shape of the 1128-keV γ ray is suggestive of a broadened shape, consistent with simulations of a delayed emission with a mean life of around 50 ps. However, the effects are not strong enough to provide evidence. Proof of a delayed emission will have to come from a recoil-distance method measurement. Such a measurement would provide a strong confirmation of the deformed nature of this state, its microscopic configuration, and, thus, triple configuration coexistence in this nuclide.

In summary, we have examined configuration coexistence in ^{44}S using the two-proton knockout reaction from ^{46}Ar at intermediate energy. Four new excited states were observed. Two new spin assignments were made based on the longitudinal momentum distributions of the projectile residues. The observed states include a 4^+ state at 2447 keV. A shell-model calculation using the SDPF-U interaction suggests that this state has a strong prolate deformation in both the laboratory and intrinsic frames, but that its deformation is based on a neutron 1p-1h configuration which is different from the neutron 2p-2h intruder configuration responsible for the ground-state deformation of this nucleus. A recoil-distance method measurement of the lifetime of the 2447-keV 4^+ state could confirm its deformed nature and the presence of triple configuration coexistence within 2.4 MeV in ^{44}S.

This work was supported by the National Science Foundation under Grants No. PHY-0606007, No. PHY-0355129, No. PHY-0653323, No. PHY-0758099, and No. PHY-0754674, by the US Department of Energy under Contract No. DE-FG02-02ER41220, and by the United Kingdom STFC and EPSRC under Grants No. ST/F012012 and No. EP/P503892/1. A.G. is supported by the Alfred P. Sloan Research Foundation.

[1] T. R. Werner *et al.*, Phys. Lett. B **333**, 303 (1994).
[2] T. R. Werner *et al.*, Nucl. Phys. A **597**, 327 (1996).
[3] J. Terasaki, H. Flocard, P.-H. Heenen, and P. Bonche, Nucl. Phys. A **621**, 706 (1997).

[4] G. A. Lalazissis, A. R. Farhan, and M. M. Sharma, Nucl. Phys. A **628**, 221 (1998).
[5] G. A. Lalazissis, D. Vretenar, P. Ring, M. Stoitsov, and L. Robledo, Phys. Rev. C **60**, 014310 (1999).
[6] S. Peru, M. Girod, and J. F. Berger, Eur. Phys. J. A **9**, 35 (2000).
[7] R. Rodriguez-Guzman, J. L. Egido, and L. M. Robledo, Phys. Rev. C **65**, 024304 (2002).
[8] J. Piekarewicz, J. Phys. G **34**, 467 (2007).
[9] T. Otsuka *et al.*, Phys. Rev. Lett. **104**, 012501 (2010).
[10] N. A. Smirnova *et al.*, Phys. Lett. B **686**, 109 (2010).
[11] L. Gaudefroy *et al.*, Phys. Rev. Lett. **97**, 092501 (2006).
[12] A. Gade *et al.*, Phys. Rev. C **71**, 051301(R) (2005).
[13] C. M. Campbell *et al.*, Phys. Rev. Lett. **97**, 112501 (2006).
[14] B. Bastin *et al.*, Phys. Rev. Lett. **99**, 022503 (2007).
[15] L. A. Riley *et al.*, Phys. Rev. C **78**, 011303(R) (2008).
[16] C. Force *et al.*, Phys. Rev. Lett. **105**, 102501 (2010).
[17] F. Nowacki and A. Poves, Phys. Rev. C **79**, 014310 (2009).
[18] D. J. Morrissey *et al.*, Nucl. Instrum. Methods Phys. Res. B **204**, 90 (2003).
[19] D. Bazin *et al.*, Nucl. Instrum. Methods Phys. Res. B **204**, 629 (2003).
[20] W. F. Mueller *et al.*, Nucl. Instrum. Methods Phys. Res. A **466**, 492 (2001).
[21] T. Glasmacher *et al.*, Phys. Lett. B **395**, 163 (1997).
[22] D. Sohler *et al.*, Phys. Rev. C **66**, 054302 (2002).
[23] S. Grevy *et al.*, Eur. Phys. J. A **25**, 111 (2005).
[24] J. A. Tostevin, G. Podolyak, B. A. Brown, and P. G. Hansen, Phys. Rev. C **70**, 064602 (2004).
[25] J. A. Tostevin and B. A. Brown, Phys. Rev. C **74**, 064604 (2006).
[26] E. C. Simpson, J. A. Tostevin, D. Bazin, B. A. Brown, and A. Gade, Phys. Rev. Lett. **102**, 132502 (2009).
[27] E. C. Simpson, J. A. Tostevin, D. Bazin, and A. Gade, Phys. Rev. C **79**, 064621 (2009).
[28] E. C. Simpson and J. A. Tostevin, Phys. Rev. C **82**, 044616 (2010).